Biochimica et Biophysica Acta 1840 (2014) 1838–1849

Contents lists available at ScienceDirect

Biochimica et Biophysica Acta

journal homepage: www.elsevier.com/locate/bbagen

Cigarette smoke-induced alveolar epithelial–mesenchymal transition is mediated by Rac1 activation

Hui-juan Shen [a,b,1], Yan-hong Sun [b,1], Shui-juan Zhang [c], Jun-xia Jiang [a,b], Xin-wei Dong [b], Yong-liang Jia [b], Jian Shen [b], Yan Guan [b], Lin-hui Zhang [b], Fen-fen Li [b], Xi-xi Lin [b], Xi-mei Wu [b], Qiang-min Xie [b,d,*], Xiao-feng Yan [a,**]

[a] The Second Affiliated Hospital, Medical College of Zhejiang University, Hangzhou 310009, China
[b] Zhejiang Respiratory Drugs Research Laboratory of State Food and Drug Administration of China, Medical College of Zhejiang University, Hangzhou 310058, China
[c] Pharmacy College of Zhejiang Chinese Medical University, Hangzhou 310053, China
[d] Laboratory Animal Center of Zhejiang University, Hangzhou 310058, China

ARTICLE INFO

Article history:
Received 8 August 2013
Received in revised form 13 January 2014
Accepted 28 January 2014
Available online 4 February 2014

Keywords:
Epithelial–mesenchymal transition
TGF-β1
Cigarette smoke extract
Rac1
Pulmonary fibrosis

ABSTRACT

Background: Epithelial–mesenchymal transition (EMT) is the major pathophysiological process in lung fibrosis observed in chronic obstructive pulmonary disease (COPD) and lung cancer. Smoking is a risk factor for developing EMT, yet the mechanism remains largely unknown. In this study, we investigated the role of Rac1 in cigarette smoke (CS) induced EMT.
Methods: EMT was induced in mice and pulmonary epithelial cells by exposure of CS and cigarette smoke extract (CSE) respectively.
Results: Treatment of pulmonary epithelial cells with CSE elevated Rac1 expression associated with increased TGF-β1 release. Blocking TGF-β pathway restrained CSE-induced changes in EMT-related markers. Pharmacological inhibition or knockdown of Rac1 decreased the CSE exposure induced TGF-β1 release and ameliorated CSE-induced EMT. In CS-exposed mice, pharmacological inhibition of Rac1 reduced TGF-β1 release and prevented aberrations in expression of EMT markers, suggesting that Rac1 is a critical signaling molecule for induction of CS-stimulated EMT. Furthermore, Rac1 inhibition or knockdown abrogated CSE-induced Smad2 and Akt (PKB, protein kinase B) activation in pulmonary epithelial cells. Inhibition of Smad2, PI3K (phosphatidylinositol 3-kinase) or Akt suppressed CSE-induced changes in epithelial and mesenchymal marker expression.
Conclusions and general significance: Altogether, these data suggest that CS initiates EMT through Rac1/Smad2 and Rac1/PI3K/Akt signaling pathway. Our data provide new insights into the fundamental basis of EMT and suggest a possible new course of therapy for COPD and lung cancer.

1. Introduction

Smoking is one of the leading causes of lung cancer and chronic obstructive pulmonary disease (COPD). Among smokers, lung cancer and COPD commonly coexist. In addition, the presence of COPD increases the risk of developing lung cancer [1]. Strikingly, patients with pulmonary fibrosis have a significantly higher risk to develop lung cancer and COPD. EMT has been reported as a source of increased fibroblast proliferation in diseases [2]. EMT occurs commonly in smokers and is associated with airway inflammation in lung cancer and COPD as described nearly 30 years ago [3,4]. Recently, EMT has been suggested as a potential source for lung fibrosis [5]. It plays an important role in repairing and scar formation following epithelial injury. Furthermore, previous studies have shown that fibrotic remodeling caused by EMT is one of the major contributors to life-threatening organ dysfunction in chronic lung diseases such as COPD and lung cancer [6].

COPD and lung cancer have been considered the result of ongoing inflammation and cellular injury that follow the subsequent activation and proliferation of resident mesenchymal elements in the lung [7]. Chronic airway inflammation caused by CS contributes to alterations in the bronchial epithelium and lung microenvironment, provoking a milieu conducive to pulmonary carcinogenesis. For example, CS-inducible transforming growth factor β1 (TGF-β1) is upregulated in non-small cell lung cancer and also plays an important role in promoting EMT [8].

Abbreviations: EMT, epithelial–mesenchymal transition; COPD, chronic obstructive pulmonary disease; CSE, cigarette smoke extract; TGF-β1, transforming growth factor β1; α-SMA, α-smooth muscle actin; MMP-9, matrix metalloproteinases-9; ATNA, anti-TGF-β1 neutralizing antibody; NSC, NSC23766, Rac1 inhibitor; Erk, extracellular regulated protein kinases; MAPK, mitogen-activated protein kinases; Akt, PKB, protein kinase B; ALK5, the activin receptor-like kinase 5; PI3K, phosphatidylinositol 3-kinase; JNK, c-Jun N-terminal kinases

* Correspondence to: Q. Xie, Medical College of Zhejiang University, # 866 Yuhangtang Rd, Hangzhou 310058, China. Tel.: +86 571 8820 8231; fax: +86 571 8820 8070.
** Correspondence to: X. Yan, Medical College of Zhejiang University, # 88 Jiefang Rd, Hangzhou 310009, China. Tel.: +86 571 87784529; fax: +86 571 87783898.
E-mail addresses: xieqm@zju.edu.cn (Q. Xie), yanxiaofeng0804@sina.com (X. Yan).
[1] These authors contributed equally to this work.

0304-4165/$ – see front matter © 2014 Elsevier B.V. All rights reserved.
http://dx.doi.org/10.1016/j.bbagen.2014.01.033

Milara and colleagues recently provide evidence of an active EMT process in the small bronchi of smokers and patients with COPD which may potentially contribute to the thickening of the wall of the small airways. Their studies show that cigarette smoke may induce EMT, modulating the TGF-β1 pathway as well as ROS and cAMP levels in human bronchial epithelial cells (HBECs) [9]. Increased cAMP level reduced ROS, TGF-β1 secretion and their downstream signaling phospho-ERK1/2 and phospho-Smad3 as well as the EMT process [10]. Cigarette smoke contains a high number of ROS that may activate latent TGF-β1 release, activating its downstream signaling Smad2/3 cascade in bronchial rat explants to promote small bronchi remodeling in vivo [11]. In vitro, exposure to CSE causes an EMT-like phenotype by inducing certain changes of gene and protein expression [12,13]. TGF-β1, a potent inducer of EMT, has been shown to mediate EMT in several different cell lines including alveolar and bronchial epithelial cells. In epithelial cells, TGF-β1-induced EMT is mediated by several downstream factors such as ROS generation, activation of MAPK (mitogen-activated protein kinase) and Smad signaling [14]. In vivo evidence for TGF-β1-mediated EMT has also been reported, confirming the master regulation role of TGF-β1 [2]. Thus, blocking TGF-β1 pathway directed at attenuating EMT, such as inhibitors, antibodies, ligand traps, antisense oligos, ALK5 (the activin receptor-like kinase 5) inhibitors, and immune response-based strategies [15]. However, whether blocking TGF-β1 pathway can attenuate CSE-induced EMT remains a future study. More recently, novel mechanisms of epigenetic control, alternative splicing, miRNAs, translation control, and posttranslational modifications have been shown to play key roles in the control of EMT [16]. However, the mechanism regarding how CSE mediates EMT-like changes and the signaling events that underlie EMT are not fully understood. Additional research is required to investigate the role of EMT in chronic inflammatory lung diseases and lung carcinogenesis.

Rac1 is known to be overexpressed in most cancers [17]. Depletion of Rac1 strongly inhibits cell migration and invasion by carcinoma cells. Thus, pharmacological inhibition of Rac1 may represent a novel approach to inhibit fibrosis [18]. Although a significant number of studies have analyzed the role of Rho pathways in TGF-β1-induced transformation, very little is known about the regulation of Rho GTPases by CSE as well as their subsequent contribution to EMT. Rac1, a member of the Rho family of small GTPases, is required for fibroblast migration as demonstrated both in vitro and in vivo [19,20]. Knocking out Rac1 in mice prevents the formation and inhibits the function of myofibroblasts. Furthermore, it delays cutaneous tissue repair and promotes resistance to bleomycin-induced fibrosis, thus providing opportunities to investigate therapeutic interventions [21,22]. Akt pathway is also involved in Rho family signal transduction and is known to affect cell migration [23,24]. A variety of stimuli such as hormones, growth factors, and ECM can activate the Akt signaling pathway in cells [19,25]. PI3K and Akt have a great impact on a variety of cellular processes such as cell survival, migration, cytoskeletal remodeling and metabolic control [26]. Whether Rac1, PI3K, and Akt participate in CSE induced EMT has not been investigated.

In this study, we tested the hypothesis that inhibition of Rac1 may reverse CSE-induced EMT in human type II alveolar epithelial cells. The role of Rac1 in regulating EMT was confirmed in a mouse model of CS exposure that is accompanied with characteristic EMT events. We attempted to identify signaling pathways that are involved in CSE-induced Rac1 activation and their roles in CSE-mediated Smad,

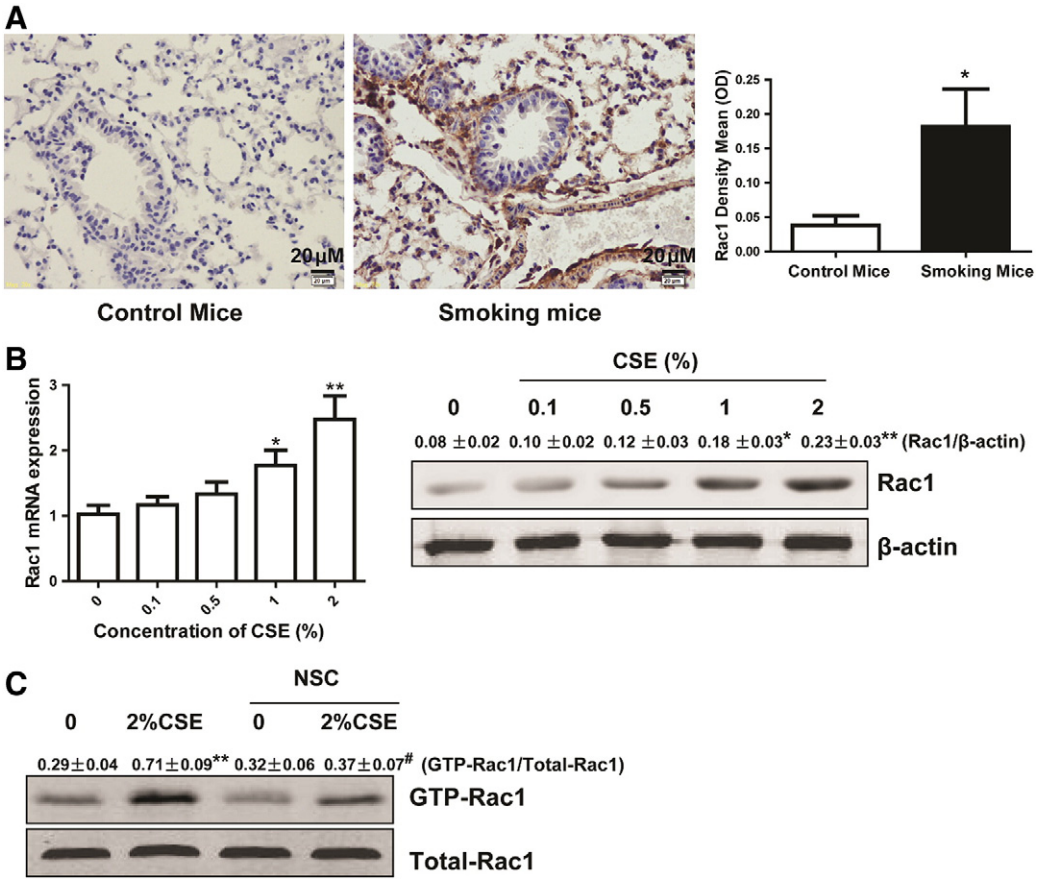

Fig. 1. CS upregulates level of Rac1 in lung tissues of a mouse model and pulmonary epithelial cell culture. (A) Rac1 expression is shown in lung tissues from mice exposed to CS or laboratory air (control). Data represent means ± S.E.M. from 4 independent experiments. Scale bar, 20 μm. 0, not treated with CSE. $^{*}p < 0.05$, compared with control. (B) A549 cells were treated with CSE for 48 h. Cells were harvested to measure Rac1 gene expression by real-time PCR (n = 4 per group) and Rac1 protein production by immunoblotting (n = 3 per group). Data represent mean ± S.E.M. $^{*}p < 0.05$ and $^{**}p < 0.01$, compared with untreated group. (C) A549 cells were pretreated with 20 μM NSC for 0.5 h and then exposed to 2% CSE for 0.5 h. Cell lysates were then immunoprecipitated. Data represent means ± S.E.M. from three independent experiments. $^{**}p < 0.01$ compared with untreated group. $^{\#}p < 0.05$ compared with 2% CSE treated group.

PI3K/Akt and p38 MAPK activation. Our data provide new insights into the fundamental basis of EMT and suggest a possible new course of therapy for COPD and lung cancer.

2. Materials and methods

2.1. Materials

High glucose-DMEM, FBS, penicillin, and streptomycin were obtained from Thermo Fisher Scientific (Kalamazoo, MI). Anti-TGF-β1 neutralizing antibody (ATNA) and ALK5 inhibitor (SB43152) were purchased from Sigma-Aldrich (St. Louis, MO). PI3 kinase inhibitor (Ly294002), Akt inhibitor (MK-2206 dihydrochloride) and p38 inhibitor (SB203580) were obtained from Santa Cruz Biotechnology (Santa Cruz, CA).

2.2. Animals

Wild-type (WT) C57BL/6 mice (weighing 20 ± 2 g) were purchased from Shanghai Slac Laboratory Animal Co. Ltd (NO. SCXK 2012–0002). All animals were housed in Plexiglas cages, kept on a 12/12-h light–dark cycle and received food and water ad libitum in temperature- and humidity-controlled rooms. To investigate the treatment effects of NSC (Tocris, USA) on EMT, mice were pretreated with NSC by an i.p. injection at concentrations of 2.5 mg/kg dissolved in saline 0.5 h before CS exposure for 10 d. An equal volume of saline was substituted for the NSC in the model group and control group, respectively. After the treatment, the animals were placed in a plastic box and exposed to CS.

2.3. Animal exposures

The mice were exposed to whole-body CS generated from research-grade cigarettes (3R4F; University of Kentucky, Lexington, KY) in 5-l smoking chambers for 10 d, the method of which was modified according to previous research [27]. Mice were exposed to 9 cigarettes/day (control mice were exposed to laboratory air). The lung tissue and bronchoalveolar lavage fluids (BALFs) were collected 18 h after the last CS exposure.

2.4. Tissue processing and immunohistochemistry analysis

The left lung of each mouse was embedded in paraffin using standard procedures. Sections (5 μm) were mounted on slides for IHC and Masson's trichrome stain analysis. IHC analysis was performed using an indirect method with antibody against the S100A4 protein (Abcam, Cambridge, MA, USA) or the Rac1 protein (Cell Signaling Technology, Danvers, MA), and the following stain was applied: Masson's trichrome stain for collagen. All specimens were measured using DP2-BSW software (Olympus, Tokyo, Japan).

2.5. Cell culture

A549 cells were purchased from American Type Culture Collection and continuously maintained at 37 °C in a 5% CO_2 atmosphere in high glucose-DMEM containing 10% fetal bovine serum (FBS), 2 mM L-glutamine, 100 U/ml penicillin and 100 μg/ml streptomycin.

2.6. Preparation of cigarette smoke extract

Research-grade cigarettes (3R4F) were obtained from the Kentucky Tobacco Research Council (University of Kentucky, Lexington, KY). The composition of 3R4F research grade cigarettes was as follows: total particulate matter (10.9 mg/cigarette), tar (9.4 mg/cigarette), and nicotine (0.726 mg/cigarette). CSE was prepared by bubbling smoke from three cigarettes into 30 ml PBS according to our previous method [27].

2.7. RNA isolation and quantitative PCR

Total RNA was extracted with the TRIZOL reagent (Takara, Otsu, Shiga, Japan) according to the manufacturer's instructions. The PCR primers were purchased from Shanghai Bioengineering Ltd (Shanghai, China). After PCR reactions, the products were subjected to 1.5% agarose

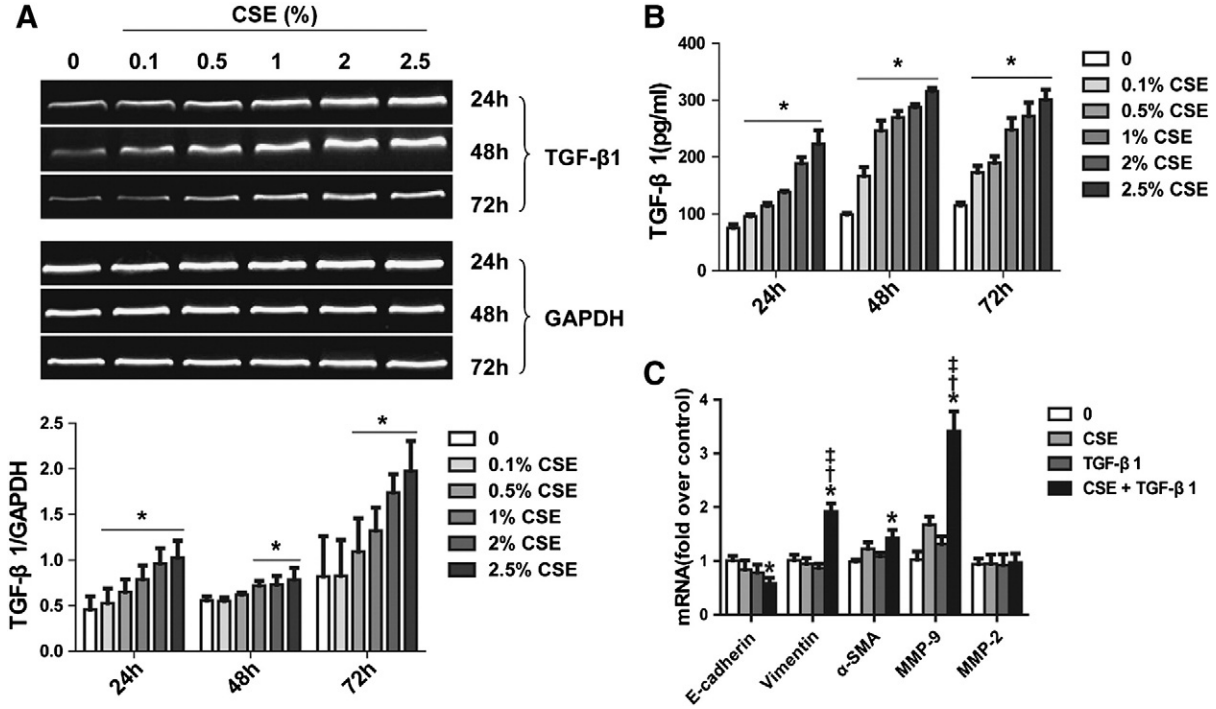

Fig. 2. CSE increases TGF-β1 expression in human type II alveolar epithelial cells. CSE upregulates TGF-β1 mRNA (A) and protein level (B) following CSE stimulation in a concentration- and time-dependent manner in A549 cells. (C) Expression changes of EMT-related markers following 48 h 0.1% CSE + 0.5 ng/ml TGF-β1 in A549 cells. Data represent mean ± S.E.M. from 4 independent experiments. 0, not treated with CSE. $^{*}p < 0.05$ compared with untreated group. $^{\dagger}p < 0.05$ compared with CSE group. $^{\ddagger}p < 0.05$ compared with TGF-β1 group.

gel electrophoresis and stained with ethidium bromide. All primers were checked against BLAST for selectivity. Real-time PCR cycling was carried out (Real-time PCR system 7500; Applied Biosystems) under the following conditions: denaturation at 95 °C for 10 s, annealing at 60 °C for 15 s, and extension at 72 °C for 30 s. An initial denaturation step at 95 °C for 5 min and a final extension step at 72 °C for 10 min were also included. PCR was performed for 40 cycles. β-actin was amplified as an internal control. The mRNA levels were calculated using the comparative parameter threshold cycle (Ct) and normalized top-actin.

2.8. Measurement of TGF-β1 by ELISA

To assay the total TGF-β1 content, the BALF or the supernatants were acidified with 1 N HCl followed by subsequent neutralization with 1.2 N NaOH/0.5 M HEPES and then measured with the Quantikine TGF-β1 assay kit (R&D Systems, Minneapolis, MN) according to the manufacturer's instructions. One hundred microliters of cell supernatant or the BALF, standards, positive controls, or medium used as a negative control was incubated on a pre-coated ELISA plate along with 100 μl of buffered protein solution for 90 min. The plates were washed three times, and 100 μl of TGF-β1 conjugate was added. After incubating for 1 h, the plates were washed, and the substrate and stop solution were added. The color absorbance at 450 nm was measured using a Bio-Rad microplate reader.

2.9. Immunoblotting analysis

The distal portion of mouse lung tissues or cells were homogenized in RIPA buffer (150 mM NaCl; 50 mM Tris, pH 8.0; 1% Triton X-100; 0.5% sodium deoxycholate; and 0.1% SDS, supplemented with protease and phosphatase inhibitors) before further analysis. Lysates of whole lung tissues or cells (30 μg) were separated by SDS-PAGE and immunoblotted using antibodies against the following proteins: α-smooth muscle actin (α-SMA) and β-actin (Bioworld, St. Louis Park, MN); E-cadherin, vimentin, Smad2, p-Smad2, P38, p-P38, AKT, and p-AKT (Cell Signaling Technology, Danvers, MA, USA). Immunoreactive bands were visualized by a two-color infrared imaging system (Odyssey, LICOR, USA).

2.10. Rac activity assay

Rac activity was measured using a Rac activity assay kit (Thermo, USA). The assay was performed according to the manufacturer's instructions. Briefly, epithelial cells were grown in 100 mm dishes and protein was harvested by 1× Lysis/Binding/Wash Buffer containing

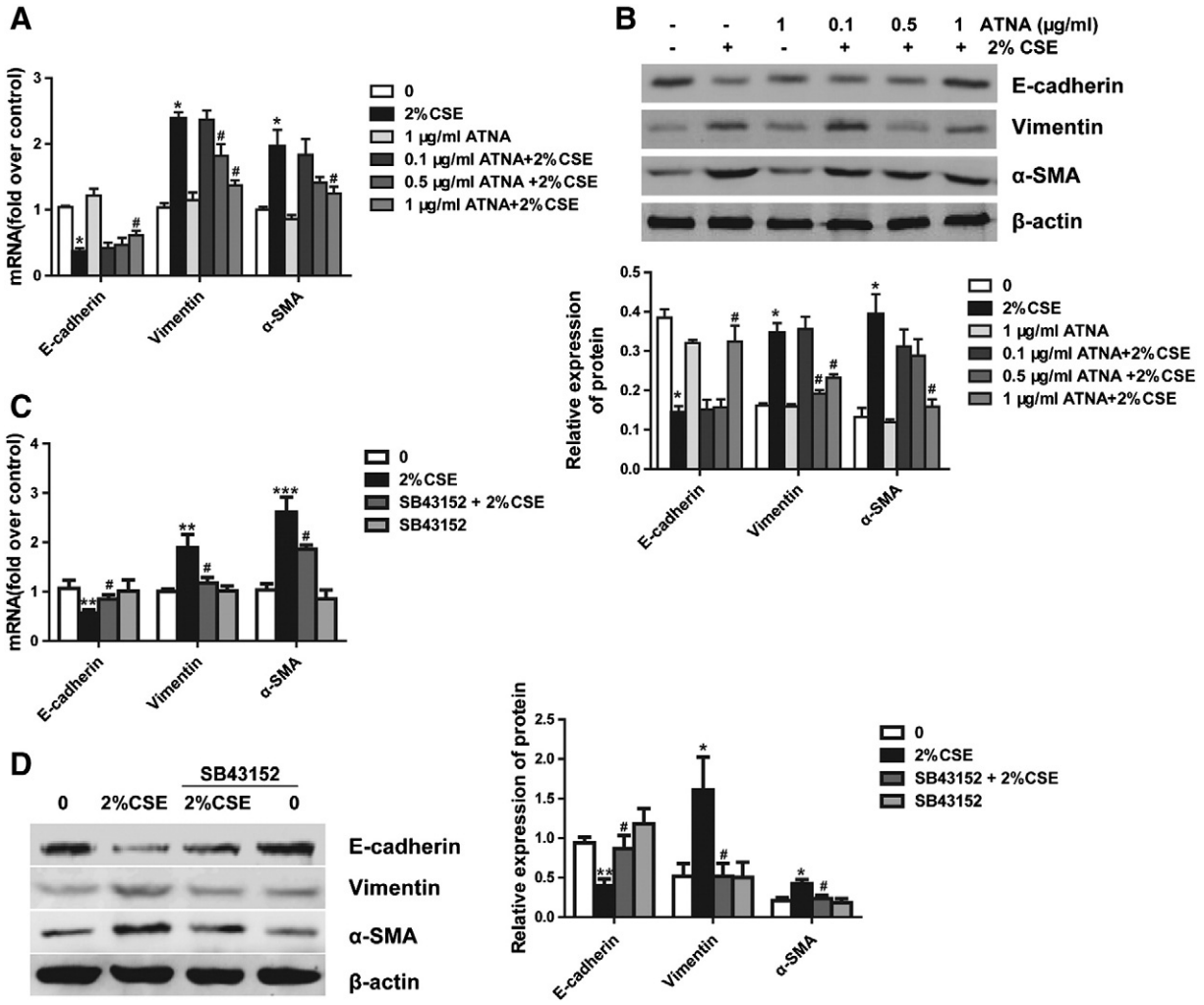

Fig. 3. Effects of incubation of ATNA (0.1, 0.5, or 1 μg/ml) on CSE-induced EMT-related markers mRNA (A) and protein expression (B) in A549 cells. The down-regulation of E-cadherin and the up-regulation of vimentin, α-SMA mRNA and protein expressions are blocked by 10 μM SB43152 (C and D). Data represent mean ± S.E.M. from 4 independent experiments. 0, not treated with CSE. $^{*}p < 0.05$, $^{**}p < 0.01$, $^{***}p < 0.001$ compared with untreated group. $^{\#}p < 0.05$ compared with cells treated with 2% CSE group.

PMSF. Glutathione Resin, to which a GST-human Pak1-PBD fusion protein was conjugated, and active Rac (Rac-GTP), which binds GST-human Pak1-PBD, were recovered through repeated centrifugation and washing of the Glutathione Resin. Bound Rac was identified by boiling beads in 2× SDS Sample Buffer and subjecting the resultant extracts to SDS-PAGE and Western blot analysis using an anti-Rac antibody.

2.11. Rac1/Smad2 siRNA preparation and transfection

Rac1/Smad2-specific siRNA were purchased from GenePharma (Shanghai, China). The cells were cultured in a 6-well plate for 24 h. Then, the Rac1/Smad2-specific or control siRNA was transfected into epithelial cells by using Lipofectamine 2000 (Invitrogen, CA) according to the manufacturer's instructions. Immunoblotting analysis was used to examine Rac1/Smad2 silencing by siRNA at 48 h after transfection.

2.12. Statistical analysis

The data were expressed as the means ± S.E.M. Statistical tests were performed using SPSS software (version 16.0, SPSS Inc., Chicago, IL, USA). One-way Analysis of Variance (ANOVA) followed by the Student–Newman–Keuls test was used to determine multiple comparisons. Statistical significance was accepted at $P < 0.05$.

3. Results

3.1. CS elevated Rac1 expression in vivo and in vitro

We showed in Fig. 1A that CS elevated Rac1 expression in lung tissues in vivo. On the other hand, we confirmed that 48 h exposure of A549 cells to CSE triggered increases in Rac1 mRNA and protein expression in a concentration-dependent manner (Fig. 1B). In addition, stimulation of A549 cells with CSE activated Rac1, which can be suppressed by NSC (Fig. 1C). These data suggest that Rac1 signaling is responding to CS and may participate in CS-mediated EMT.

3.2. CSE increases TGF-β1 level in epithelial cells in vitro

It has been demonstrated in vitro that TGF-β1 can mediate EMT in a number of epithelial cells, including renal proximal tubular, lens, and alveolar epithelial cells [28]. We next investigated the effect of CSE on TGF-β1 level in A549 cells. We found that CSE increased TGF-β1 mRNA (Fig. 2A) and protein production (Fig. 2B) in A549 cells in a concentration- and time-dependent manner. We have tried to apply TGF-β1 (0.5 ng/ml) based on previous reports [7,29], but failed to induce the expected EMT-related changes. Therefore, we used a combination of TGF-β1 (0.5 ng/ml) and 0.1% CSE to induce EMT in pulmonary epithelial cells and measured changes in expression of EMT-related markers by Q-PCR. As depicted in Fig. 2C, our findings revealed that co-incubation with 0.1% CSE and 0.5 ng/ml TGF-β1 for 48 h caused a significant decrease in expression of E-cadherin and an increase in expression of vimentin, α-SMA, and MMP-9 mRNA levels; however, the change in expression of MMP-2 was not statistically significant.

To further confirm the critical role of TGF-β signaling in CSE-induced EMT, we treated cells with ATNA to prevent the binding of active TGF-β to its type II receptor and consequently block downstream signaling. This approach prevented the down-regulation of E-cadherin and the up-regulation of vimentin, α-SMA mRNA and protein expression in CSE-induced EMT (Fig. 3A and B). Meanwhile, we employed an ALK5-specific inhibitor (10 μM SB43152) to corroborate the participation of TGF-β in CSE-induced EMT. The down-regulation of E-cadherin and the up-regulation of vimentin, α-SMA expressions were in a fashion restrained by ALK5 inhibition (Fig. 3C and D). These observations indicate that CSE induced EMT through TGF-β and its downstream signaling activation.

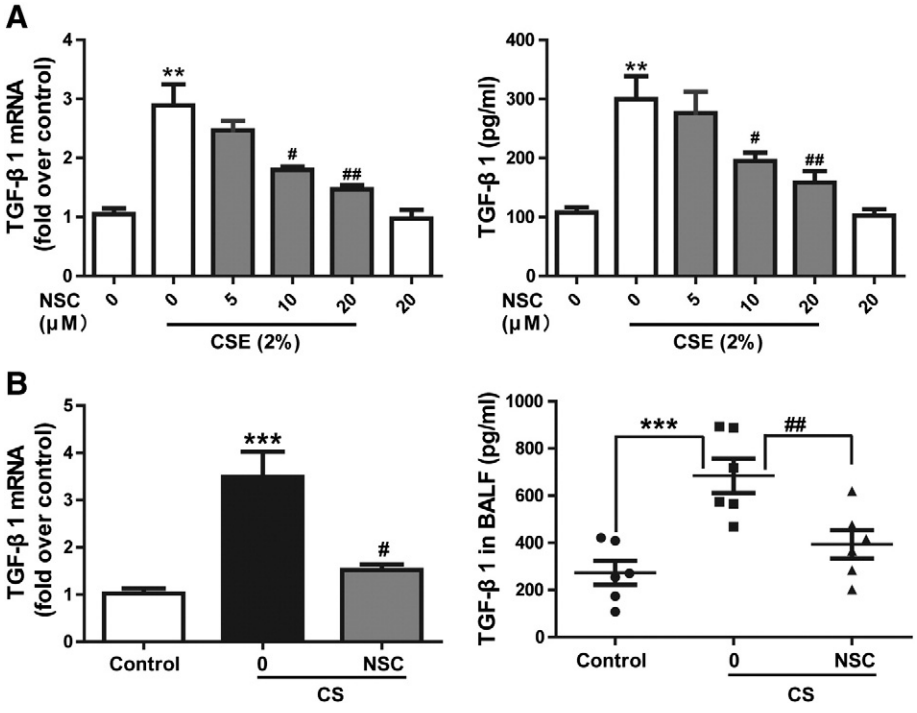

Fig. 4. NSC suppresses CSE-induced TGF-β1 release in pulmonary epithelial cells and CS mouse models. (A) A549 cells were pretreated with NSC (5–20 μM) for 30 min; then, the cells were stimulated with 2% CSE for 48 h. After stimulation with CSE, cell culture media were collected to measure TGF-β1 protein by ELISA, and the cells were harvested for TGF-β1 gene expression by real-time PCR (n = 4 per group). (B) C57BL/6 mice were repeatedly exposed to CS for 10 d. Mice were treated with NSC (2.5 mg/kg) by i.p. injection at 30 min before daily CS exposure. At 18 h after the last CS exposure, BALFs were harvested to measure TGF-β1 release by ELISA. Lung tissues were harvested for TGF-β1 gene expression by real-time PCR (n = 6 per group). Data represent mean ± S.E.M. 0, not treated with CSE or not treated with NSC. $^{**}p < 0.01$, $^{***}p < 0.001$ compared with untreated group. $^{\#}p < 0.05$, $^{\#\#}p < 0.01$ compared with CSE-stimulated cells or mice with CS exposure.

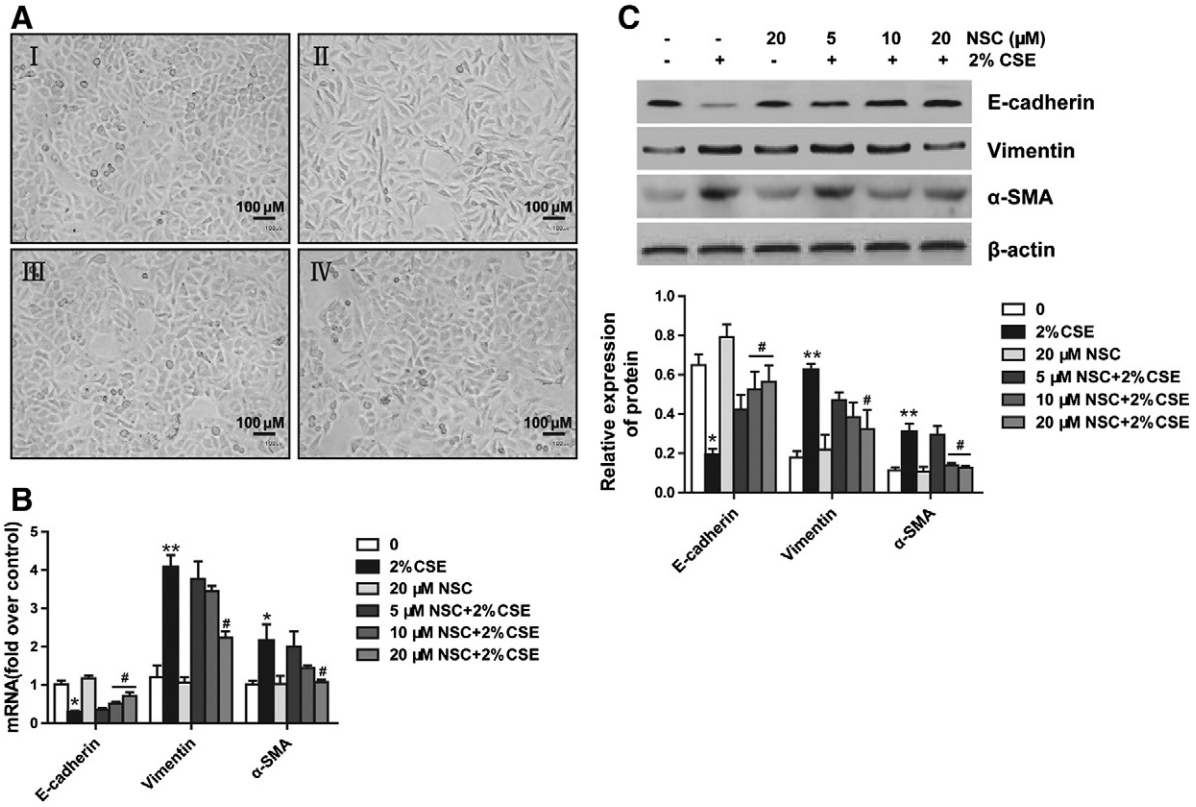

Fig. 5. Effects of NSC on CSE-induced EMT in pulmonary epithelial cells. A549 cells were pretreated with or without NSC (5, 10, or 20 μM) for 0.5 h and then exposed to 2% CSE for 48 h. AI: control cells in media alone have a pebble-like shape and display cell-cell contacts consistent with an epithelial morphology. AII: cells treated with 2% CSE exhibit a fibroblast-like morphology with cellular elongation and reduction of cell-cell contacts. AIII: treatment with 20 μM NSC alone causes no appreciable changes in cell morphology. AIV: 20 μM NSC prevents changes induced by CSE and preserves an epithelial morphology (Images were obtained by confocal microscopy, magnification of 10×). E-cadherin, vimentin and α-SMA mRNA expression was measured by real-time PCR (B), and E-cadherin, vimentin and α-SMA protein expression was measured by immunoblotting (C). Data represent mean ± S.E.M. from 4 independent experiments. 0, not treated with CSE. $^{*}p < 0.05$, $^{**}p < 0.01$ compared with untreated group. $^{\#}p < 0.05$ compared with cells treated with 2% CSE.

3.3. Pharmacological suppression of Rac1 alleviates TGF-β1 production in CS-exposed mice

To assess potential role of Rac1 in regulating EMT, we examined effects of CSE on TGF-β1 gene expression and protein production in pulmonary epithelial cells with administration of NSC, a Rac1 inhibitor. As shown in Fig. 4A, pharmacological inhibition of Rac1 results in marked reduction of TGF-β1 in both mRNA and protein levels. To further probe effects of Rac1 inhibition on CS exposure in vivo, C57BL/6 mice were exposed to CS or laboratory air for 10 d consecutively. CS-model mice were i.p. injected with NSC (2.5 mg/kg), 30 min before quotidian CS exposure. Lung tissues were harvested 18 h after the last CS exposure. Our findings suggested that TGF-β1 release was significantly reduced in NSC-pretreated mice (Fig. 4B). These observations suggest a potential role of Rac1 in TGF-β1-modulated EMT in a mouse model of CS.

3.4. Inhibiting either the activity or expression of Rac1 suppresses CSE-induced EMT

Changes in cell morphology and expression of mesenchymal and epithelial markers were read out to assess the effects of NSC on CSE-induced EMT in A549 cells. Control A549 cells in media alone showed a pebble-like shape and cell–cell adhesion (Fig. 5AI). After treatment with 2% CSE, epithelial cells displayed a decrease in cell–cell contacts and adopted a more fibroblast-like morphology (Fig. 5AII). Cells treated with 20 μM NSC in the presence or absence of 2% CSE retained their pebble-like shape and displayed cell–cell adhesion consistent with retention of the epithelial phenotype (Fig. 5AIII and IV).

We next examined the effects of NSC on CSE-induced expression of mesenchymal and epithelial markers in A549 cells. Real-time PCR analysis showed an expected decrease in E-cadherin mRNA expression and increases in vimentin and α-SMA expression 48 h after exposure to 2% CSE compared with untreated groups. Cells pretreated with the Rac1-specific inhibitor NSC (5–20 μM) showed enhanced E-cadherin expression and reduced vimentin, α-SMA mRNA expression (Fig. 5B). Similar results were obtained when protein expression was assessed using immunoblotting analysis; Co-incubation of NSC (5–20 μM) with 2% CSE significantly enhanced E-cadherin protein expression and reduced vimentin, α-SMA protein expression compared with CSE treatment alone (Fig. 5C). NSC itself did not appreciably affect mRNA and protein expression in untreated of A549 cells.

To circumvent issue regarding drug specificity and solidify the conclusion, siRNA was employed to silence Rac1 gene expression in A549 cells. Immunoblotting analysis confirmed that Rac1 protein expression was significantly suppressed by Rac1 siRNA gene silencing (Fig. 6A). Most importantly, Rac1 knockdown restored the E-cadherin, vimentin, and α-SMA expression levels that were altered following CSE stimulation (Fig. 6B and C). Our data suggest that activation of Rac1 signaling pathway is required for CSE-mediated EMT.

3.5. NSC inhibits CS-induced EMT in the mouse model in vivo

The observation that NSC alleviated EMT induced by CS was further investigated in mice with pharmacological inhibition of Rac1. Effects of NSC on EMT-related markers were assessed on day 10 after CS operation. CS induced a substantial decrease in E-cadherin expression and increases in vimentin, α-SMA expression in lung tissues of CS-exposed

mice. NSC (2.5 mg/kg) treatments significantly reduced the changes (Fig. 7A and B). Sl00A4 was assessed in response to CS challenge by immunohistochemistry. Sl00A4 was widely expressed in lung tissues of CS-exposed mice, which was not seen in mice exposed to laboratory air. Furthermore, the change can be reversed by pre-treatment of NSC (Fig. 7C). Assessments of Masson's trichrome-stained lung tissues showed the Rac1-dependent effects on lung fibrosis. It was shown that CS operation induced extensive collagen deposition in the lung, which was markedly ameliorated by administration of NSC (Fig. 7D).

3.6. EMT is mediated by Rac1 signaling through Smad and PI3kinase/Akt pathway

We then further explored molecular mechanisms underlying of the regulatory function of Rac1 in CS-induced EMT. Immunoblotting analysis of the resultant protein, whole cell extracts revealed that inhibition of either the activity or expression of Rac1 suppressed CSE-induced Smad2, Akt activation, whereas P38 activation cannot be restrained by silencing or inhibiting Rac1 (Fig. 8A–C).

We then investigated the effects of inhibition on CSE-mediated perturbation of E-cadherin and vimentin expression in pulmonary epithelial cells. To test this hypothesis, we screened Smad2 siRNA, PI3 kinase inhibitor Ly294002, Akt inhibitor MK-2206 dihydrochloride, p38 inhibitor SB203580, Erk (extracellular regulated protein kinases) inhibitor U0126 or JNK (c-Jun N-terminal kinases) inhibitor SP600125 in CSE-stimulated pulmonary epithelial cells. We showed that treatment with SB203580 (Fig. 9A), U0126 or SP600125 (data not shown) cannot prevent the phenomenon, only Smad2 siRNA, Ly294002 and MK-2206 dihydrochloride suppressed the alteration of E-cadherin and vimentin expression induced by CSE stimulation (Fig. 9B–D). Thus, these results indicate that CSE-exposure induced EMT is activated by Rac1 activation through Smad2 and PI3kinase/Akt signaling pathway but not MAP kinases.

4. Discussion

In this article, we report that the inhibition of Rac1 in pulmonary epithelia prevents the EMT induced by CS via activation of the Smad2 and PI3K/Akt signaling. These findings enable us to understand a novel biological role of the Rac1 in the pathogenesis of pulmonary EMT.

Our research has focused on the role of Rac1 in lung EMT responses triggered by CS. We employed a 10 day cigarette exposure in mice as the model. This is based on our pilot experiments, where mice were exposed to cigarette for 5, 10, 20 and 30 days. We found that the most significant changes of E-cadherin, vimentin, and α-SMA protein expression have been found within the 10 day group (see supplementary Fig. 3). We found increased expression and activation of Rac1 in lung tissues of mice with CS-induced EMT responses (Fig. 1A). Similarly, CSE elevated Rac1 expression and activated the Rac1 in A549 cells (Fig. 1B and C). These findings suggest that Rac1 may be involved in the pathogenesis of EMT induced by CS in the lung. Consistent with previous reports [9,13,14], we observed that CSE promoted EMT through the activation of intracellular ROS (see supplementary Fig. 2), the release of TGF-β1, and a greater elevation of TGF-β1 expression than that of other proinflammatory cytokines and chemokines in the epithelial cells and pulmonary inflammatory of mouse model to CS. In addition, our previous data also support the increase in TGF-β expression in lung epithelial cells stimulated by CSE [30].

Pulmonary epithelia play a key role in the early defense against CSE. CSE increases TGF-β1 level or activates TGF-β1 to induce EMT, which are involved in predominant small airway fibrosis [9]. It is possible that Rac1 may regulate the CS-evoked EMT response, particularly

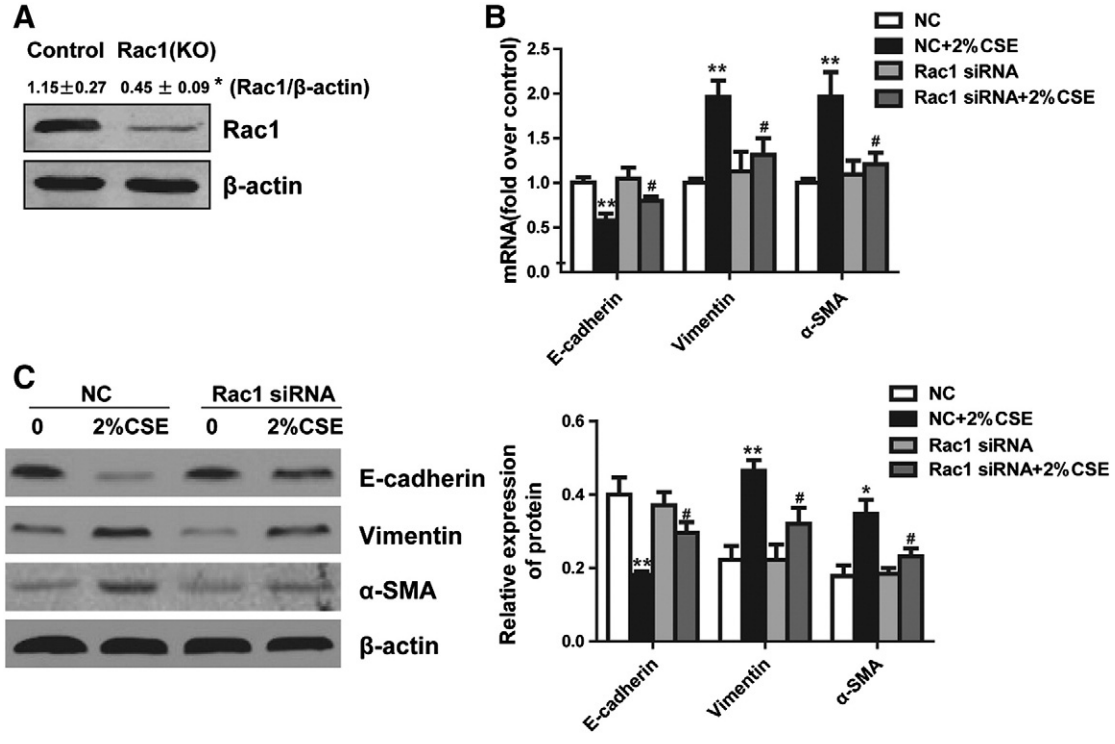

Fig. 6. Effects of Rac1 gene silencing on CSE-induced EMT in pulmonary epithelial cells. Pooled synthetic siRNA duplexes targeting different regions of Rac1 were transfected into A549 cells at 50 pmol per well. 24 h after transfection, cells were stimulated with 2% CSE in serum free 0.1% BSA/DMEM for a further 48 h prior to harvest. The cells were collected to assess the levels of Rac1 production by immunoblotting assay (A), expression changes of EMT-related markers were measured by real-time PCR and immunoblotting (B and C). Data represent mean ± S.E.M. from 4 independent experiments. 0, not treated with CSE. $^{*}p < 0.05$, $^{**}p < 0.01$ compared with negative control (NC) group. $^{\#}p < 0.05$ compared with NC + 2% CSE group.

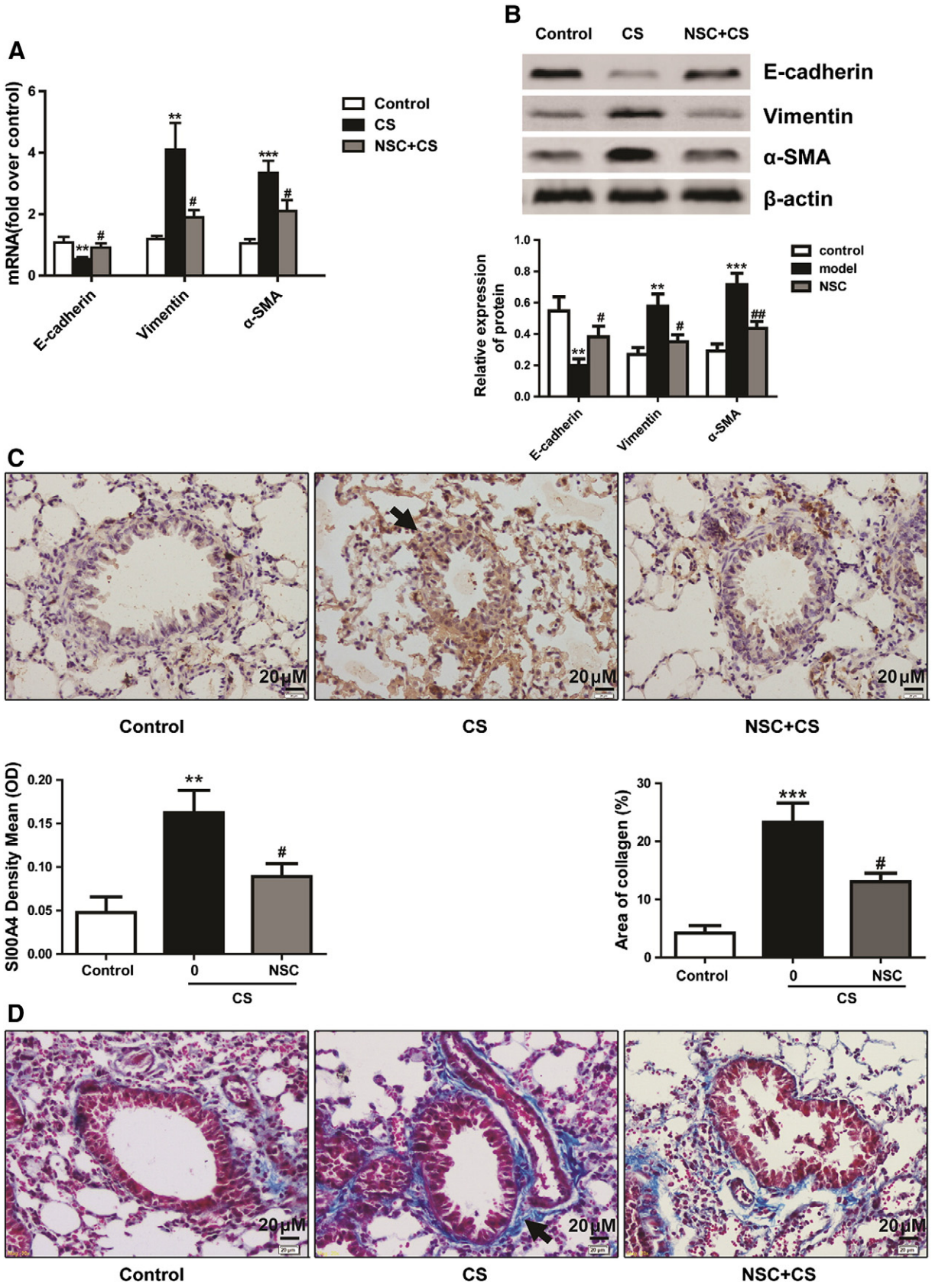

Fig. 7. NSC prevents CS-induced EMT in the mouse model. C57BL/6 mice were repeatedly exposed to CS for 10 d. Mice were treated with NSC (2.5 mg/kg) by i.p. injection at 30 min before daily CS exposure. At 18 h after the last CS exposure, lung tissues were harvested for the analysis of EMT-related markers. Expression changes of EMT-related markers were measured by real-time PCR (A) and immunoblotting (B). C: Representative photomicrographs demonstrating S100A4 expression (arrows) in lung tissue detected by immunohistochemistry. Scale bar: 20 μm. D: Representative photomicrographs demonstrating peribronchial collagen deposition (arrows) detected by Masson's trichrome staining (blue color). Scale bar: 20 μm. 0, not treated with NSC. All data shown were obtained with groups of n = 6–8 mice/group, in two separate experiments. Data represent mean ± S.E.M. $^{*}p < 0.05$, $^{**}p < 0.01$, $^{***}p < 0.001$ compared with control mice with air exposure. $^{\#}p < 0.05$, $^{\#\#}p < 0.01$ compared with control mice with CS exposure.

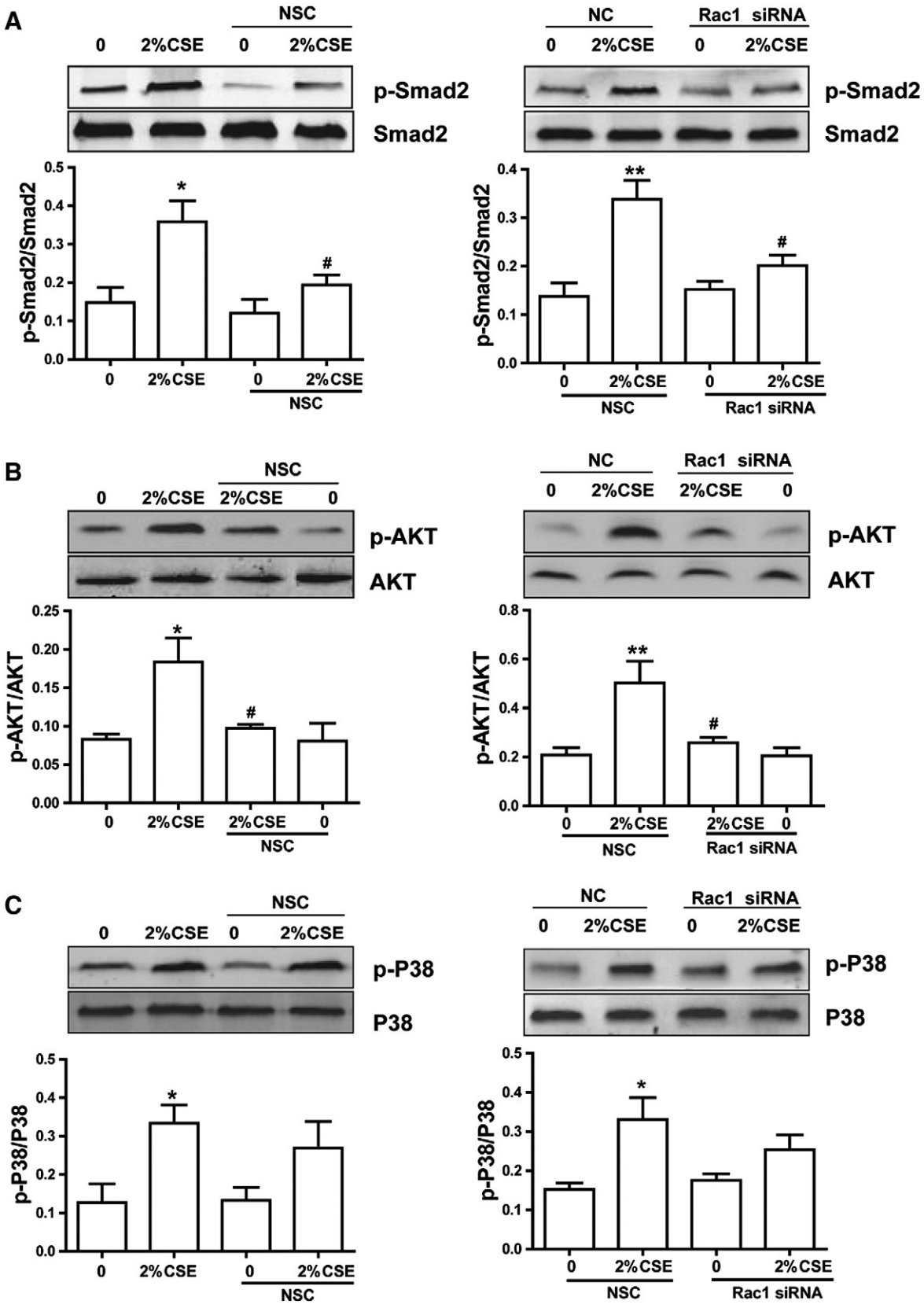

Fig. 8. Inhibiting either the activity or expression of Rac1 suppresses CSE-induced Smad2, Akt, and P38 phosphorylation in A549 cells. Cell lysates were prepared, and then immunoblotted with antibodies for phospho-Smad2 phosphorylated at Ser465/467, phospho-Akt phosphorylated at Thr-308, and phospho-p38 MAPK phosphorylated at Thr180/Tyr182. The data represent the mean ± S.E.M. from 3 independent experiments. 0, not treated with CSE. $^{*}p < 0.05$, $^{**}p < 0.01$ compared with untreated group or negative control (NC) group, $^{\#}p < 0.05$ compared with 2% CSE group or NC + 2% CSE group.

TGF-β1 expression and release. Therefore, understanding specific signaling mechanisms of EMT induced by TGF-β1 may reveal therapeutics to attenuate fibrogenesis while preserving the important homeostatic functions of TGF-β1 [31]. Our results showed that CSE stimulation increased TGF-β1 production in A549 cells (Fig. 2A and B). Furthermore, co-treatment of TGF-β1 and CSE at low concentrations strengthened their abilities to induce EMT as measured by the changes of E-cadherin, vimentin, α-SMA, and MMP-9 expression in A549 cells (Fig. 2C). To explore the underlying mechanisms, we examined whether ATNA can directly neutralize TGF-β1 and potentially be used as a therapeutic agent to suppress EMT induced by CSE. The present results showed that ATNA prevented changes in vimentin, α-SMA, and E-cadherin levels induced by CSE-stimulation (Fig. 3A and B). An ALK5-specific inhibitor (SB43152) was also used to corroborate the participation of TGF-β. The results were consistent with ATNA (Fig. 3C and D). However, through applying either ATNA or ALK5 inhibitor, blocking TGF-β did not completely prevent the CSE-mediated EMT process in our work, indicating it only partially arose from TGF-β activation in A549 cells. Other mechanisms of the EMT process could be TGF-β-independent and involving other inductors, such as MMP-9 [32], reactive oxygen species [33], IL-8 [34], or plasmin albumin [35].

In this article, we showed that inhibiting Rac1 prevented smoke-induced EMT response by increasing E-cadherin, and reducing TGF-β1 (Fig. 4B), vimentin and α-SMA mRNA (Fig. 7A) and protein expressions (Fig. 7B) as well as suppressing S100A4 protein expression (Fig. 7C) and peribronchial collagen deposition (Fig. 7D) in lung tissue in vivo. Similarly, inhibition of Rac1 significantly alleviated the morphological changes in A549 cells (Fig. 5A), increased CSE-stimulated gene expression and protein production of E-cadherin and reduced vimentin and α-SMA (Fig. 5B and C) in A549 cells in vitro. Thus, we provide novel

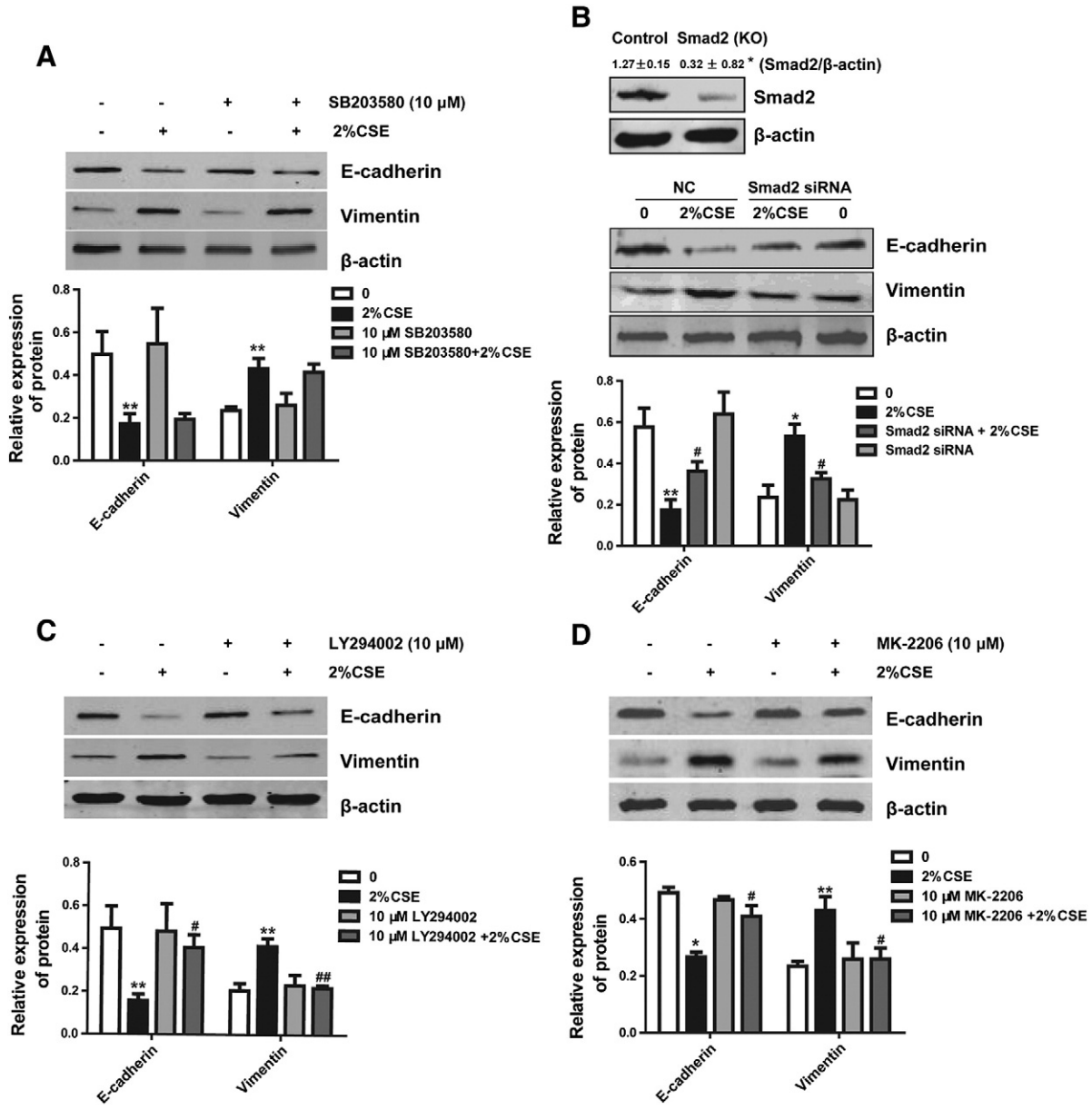

Fig. 9. Smad2 and PI3K/Akt signaling pathways are involved in CSE-mediated E-cadherin/vimentin release. A549 cells were pretreated with p38 inhibitor (10 μM SB203580), PI3 kinase inhibitor (10 μM Ly294002), or Akt inhibitor (10 μM MK-2206 dihydrochloride) for 30 min and then incubated with 2% CSE for another 48 h. Pooled synthetic siRNA duplexes targeting different regions of Smad2 were transfected into A549 cells at 50 pmol per well. E-cadherin/vimentin levels were determined by immunoblotting. Data represent mean ± S.E.M. from 3 independent experiments. 0, not treated with CSE. $^{*}p < 0.05$, $^{**}p < 0.01$ compared with untreated group or negative control (NC) group. $^{\#}p < 0.05$, $^{\#\#}p < 0.01$ compared with cells treated with 2% CSE or NC + 2% CSE group.

evidence that Rac1 regulates the lung EMT response induced by CS. This finding is further supported by studies of the genetic ablation of Rac1 on A549 cells in vitro (Fig. 6A–C).

We hypothesized that Rac1 could regulate smoke-induced lung EMT response via signaling pathways such as the Smad [9], PI3K/Akt and p38 MAPK pathway [36,37], because Rac1 positively regulates diverse cellular signaling pathways, including cytoskeletal organization, transcription and cell-cycle progression by activating the Rac1 pathway [38]. It has been suggested that Rac1 regulates PI3K/Akt signaling in response to TGF-β1, epidermal growth factor (EGF), fibroblast growth factor (FGF) and hepatocyte growth factor (HGF) in the epithelial cells [38–40]. Our data displayed that not only the phosphorylation of Smad2 and not Smad3 (data are not shown) elevated in A549 cells treated with CSE, but also the phosphorylation of Akt and p38/MAPK was increased following the expression and activation of Rac1 (Fig. 8A–C). This is an interesting phenomenon, since both Smad2 and PI3K/AKT activation seem to be dependent of Rac. Whether PI3K/AKT signaling is dependent of the increment of TGF-β or if is only dependent of increment in the expression and activity of Rac1? Therefore, we next used an ALK5-specific inhibitor (10 μM SB43152) to demonstrate whether the activation of PI3K/AKT signaling is dependent on the increment of TGF-β. We examined Akt phosphorylation. The results showed that effects of SB43152 on CSE-induced Akt phosphorylation are not statistically significant (see supplementary Fig. 4). Therefore, we speculated that the activation of PI3K/AKT signaling may be dependent on the increment in the expression and activity of Rac1. We then explored molecular mechanisms underlying the regulatory function of Rac1 in CS-induced EMT, and found that the inhibition of either the activation or expression of Rac1 suppressed CSE-induced Smad2 and Akt activation, whereas P38 activation cannot be restrained by Rac1 silencing or inhibitor (Fig. 8A–C). In order to further prove the result, we investigated the effects of some inhibitors of signaling pathway on CSE-mediated perturbation of E-cadherin and vimentin expression in pulmonary epithelial cells. We screened Smad2 siRNA, PI3 kinase inhibitor Ly294002, Akt inhibitor MK-2206 dihydrochloride, p38 inhibitor SB203580, Erk inhibitor U0126 or JNK inhibitor SP600125 in CSE-stimulated pulmonary epithelial cells. The results showed that treatment with SB203580 (Fig. 9A), U0126 or SP600125 (data not shown) cannot prevent the EMT responses, only Smad2 siRNA, Ly294002 and MK-2206 dihydrochloride suppressed the alteration of E-cadherin and vimentin expression induced by CSE stimulation (Fig. 9B–D). Thus, these results suggested that CSE-induced EMT is activated by Rac1 activation through Smad2 and PI3K/Akt signaling pathway but not MAP kinases.

This is the first study to show that CS-induced Rac1 activation can occur through recruitment of TGF-β1 in vivo and in vitro. However, whether other involving mechanisms are involved needs further study. Smoking cigarettes directly causes EMT-like changes in gene and protein expression, indicating that EMT is involved in the progression of lung cancer and COPD.

Disclosures

The authors have no financial conflicts of interest.

Acknowledgements

This work was supported by grants from the National Science Foundation of China (Nos. 30973542, 81270095 and 30772581) and the National Basic Research Program of China (No. 2009CB522103).

Appendix A. Supplementary data

Supplementary data to this article can be found online at http://dx.doi.org/10.1016/j.bbagen.2014.01.033.

References

[1] I.A. Yang, V. Relan, C.M. Wright, M.R. Davidson, K.B. Sriram, S.M. Savarimuthu Francis, B.E. Clarke, E.E. Duhig, R.V. Bowman, K.M. Fong, Common pathogenic mechanisms and pathways in the development of COPD and lung cancer, Expert Opin. Ther. Targets 15 (2011) 439–456.
[2] K.K. Kim, M.C. Kugler, P.J. Wolters, L. Robillard, M.G. Galvez, A.N. Brumwell, D. Sheppard, H.A. Chapman, Alveolar epithelial cell mesenchymal transition develops in vivo during pulmonary fibrosis and is regulated by the extracellular matrix, Proc. Natl. Acad. Sci. U. S. A. 103 (2006) 13180–13185.
[3] J. Chalon, J.S. Katz, S. Ramanathan, M. Ambiavagar, L.R. Orkin, Tracheobronchial epithelial multinucleation in malignant disease, Science 183 (1974) 525–526.
[4] M. Cosio, H. Ghezzo, J.C. Hogg, R. Corbin, M. Loveland, J. Dosman, P.T. Macklem, The relations between structural changes in small airways and pulmonary-function tests, N. Engl. J. Med. 298 (1978) 1277–1281.
[5] H.A. Chapman, Epithelial responses to lung injury: role of the extracellular matrix, Proc. Am. Thorac. Soc. 9 (2012) 89–95.
[6] R.P. Young, C.F. Whittington, R.J. Hopkins, B.A. Hay, M.J. Epton, P.N. Black, G.D. Gamble, Chromosome 4q31 locus in COPD is also associated with lung cancer, Eur. Respir. J. 36 (2010) 1375–1382.
[7] T. Walser, X. Cui, J. Yanagawa, J.M. Lee, E. Heinrich, G. Lee, S. Sharma, S.M. Dubinett, Smoking and lung cancer: the role of inflammation, Proc. Am. Thorac. Soc. 5 (2008) 811–815.
[8] J. Araya, S. Cambier, J.A. Markovics, P. Wolters, D. Jablons, A. Hill, W. Finkbeiner, K. Jones, V.C. Broaddus, D. Sheppard, A. Barzcak, Y. Xiao, D.J. Erle, S.L. Nishimura, Squamous metaplasia amplifies pathologic epithelial-mesenchymal interactions in COPD patients, J. Clin. Invest. 117 (2007) 3551–3562.
[9] J. Milara, T. Peiró, A. Serrano, J. Cortijo, Epithelial to mesenchymal transition is increased in patients with COPD and induced by cigarette smoke, Thorax 68 (2013) 410–420.
[10] J. Milara, M. Armengot, P. Banuls, H. Tenor, R. Beume, E. Artigues, J. Cortijo, Roflumilast N-oxide, a PDE4 inhibitor, improves cilia motility and ciliated human bronchial epithelial cells compromised by cigarette smoke in vitro, Br. J. Pharmacol. 166 (2012) 2243–2262.
[11] R.D. Wang, J.L. Wright, A. Churg, Transforming growth factor-beta1 drives airway remodeling in cigarette smoke-exposed tracheal explants, Am. J. Respir. Cell Mol. Biol. 33 (2005) 387–393.
[12] E. Veljkovic, J. Jiricny, M. Menigatti, H. Rehrauer, W. Han, Chronic exposure to cigarette smoke condensate in vitro induces epithelial to mesenchymal transition-like changes in human bronchial epithelial cells, BEAS-2B, Toxicol. in Vitro 25 (2011) 446–453.
[13] H. Zhang, H. Liu, Z. Borok, K.J. Davies, F. Ursini, H.J. Forman, Cigarette smoke extract stimulates epithelial-mesenchymal transition through Src activation, Free Radic. Biol. Med. 52 (2012) 1437–1442.
[14] I.E. Fernandez, O. Eickelberg, The impact of TGF-beta on lung fibrosis: from targeting to biomarkers, Proc. Am. Thorac. Soc. 9 (2012) 111–116.
[15] N. Bellam, B. Pasche, Tgf-beta signaling alterations and colon cancer, Cancer Treat. Res. 155 (2010) 85–103.
[16] Y. Katsuno, S. Lamouille, R. Derynck, TGF-beta signaling and epithelial-mesenchymal transition in cancer progression, Curr. Opin. Oncol. 25 (2013) 76–84.
[17] G. Fritz, I. Just, B. Kaina, Rho GTPases are over-expressed in human tumors, Int. J. Cancer 81 (1999) 682–687.
[18] A.Y. Chan, S.J. Coniglio, Y.Y. Chuang, D. Michaelson, U.G. Knaus, M.R. Philips, M. Symons, Roles of the Rac1 and Rac3 GTPases in human tumor cell invasion, Oncogene 24 (2005) 7821–7829.
[19] E. Wertheimer, A. Gutierrez-Uzquiza, C. Rosemblit, C. Lopez-Haber, M.S. Sosa, M.G. Kazanietz, Rac signaling in breast cancer: a tale of GEFs and GAPs, Cell. Signal. 24 (2012) 353–362.
[20] S. Liu, M. Kapoor, A. Leask, Rac1 expression by fibroblasts is required for tissue repair in vivo, Am. J. Pathol. 174 (2009) 1847–1856.
[21] J.F. Santibanez, J. Kocic, A. Fabra, A. Cano, M. Quintanilla, Rac1 modulates TGF-beta1-mediated epithelial cell plasticity and MMP9 production in transformed keratinocytes, FEBS Lett. 584 (2010) 2305–2310.
[22] S. Patel, R.M. Mason, J. Suzuki, A. Imaizumi, T. Kamimura, Z. Zhang, Inhibitory effect of statins on renal epithelial-to-mesenchymal transition, Am. J. Nephrol. 26 (2006) 381–387.
[23] K.F. Tolias, L.C. Cantley, C.L. Carpenter, Rho family GTPases bind to phosphoinositide kinases, J. Biol. Chem. 270 (1995) 17656–17659.
[24] C. Jimenez, R.A. Portela, M. Mellado, J.M. Rodriguez-Frade, J. Collard, A. Serrano, A.C. Martinez, J. Avila, A.C. Carrera, Role of the PI3K regulatory subunit in the control of actin organization and cell migration, J. Cell Biol. 151 (2000) 249–262.
[25] O. Larsson, D. Diebold, D. Fan, M. Peterson, R.S. Nho, P.B. Bitterman, C.A. Henke, Fibrotic myofibroblasts manifest genome-wide derangements of translational control, PLoS One 3 (2008) e3220.
[26] R. Williams, A. Berndt, S. Miller, W.C. Hon, X. Zhang, Form and flexibility in phosphoinositide 3-kinases, Biochem. Soc. Trans. 37 (2009) 615–626.
[27] F.F. Li, J. Shen, H.J. Shen, X. Zhang, R. Cao, Y. Zhang, Q. Qui, X.X. Lin, Y.C. Xie, L.H. Zhang, Y.L. Jia, X.W. Dong, J.X. Jiang, M.J. Bao, S. Zhang, W.J. Ma, X.M. Wu, H. Shen, Q.M. Xie, Y. Ke, Shp2 plays an important role in acute cigarette smoke-mediated lung inflammation, J. Immunol. 189 (2012) 3159–3167.
[28] V.M. Felton, Z. Borok, B.C. Willis, N-acetylcysteine inhibits alveolar epithelial–mesenchymal transition, Am. J. Physiol. Lung Cell. Mol. Physiol. 297 (2009) L805–L812.
[29] H. Kasai, J.T. Allen, R.M. Mason, T. Kamimura, Z. Zhang, TGF-beta1 induces human alveolar epithelial to mesenchymal cell transition (EMT), Respir. Res. 6 (2005) 56.

[30] Y. Guan, F.F. Li, L. Hong, X.F. Yan, G.L. Tan, J.S. He, X.W. Dong, M.J. Bao, Q.M. Xie, Protective effects of liquiritin apioside on cigarette smoke-induced lung epithelial cell injury, Fundam. Clin. Pharmacol. 26 (2012) 473–483.
[31] H.A. Chapman, Epithelial–mesenchymal interactions in pulmonary fibrosis, Annu. Rev. Physiol. 73 (2011) 413–435.
[32] Q. Yu, I. Stamenkovic, Cell surface-localized matrix metalloproteinase-9 proteolytically activates TGF-beta and promotes tumor invasion and angiogenesis, Genes Dev. 14 (2000) 163–176.
[33] N. Tobar, V. Villar, J.F. Santibanez, ROS-NFkappaB mediates TGF-beta1-induced expression of urokinase-type plasminogen activator, matrix metalloproteinase-9 and cell invasion, Mol. Cell. Biochem. 340 (2010) 195–202.
[34] X.J. Li, L.X. Peng, J.Y. Shao, W.H. Lu, J.X. Zhang, S. Chen, Z.Y. Chen, Y.Q. Xiang, Y.N. Bao, F.J. Zheng, M.S. Zeng, T.B. Kang, Y.X. Zeng, B.T. Teh, C.N. Qian, As an independent unfavorable prognostic factor, IL-8 promotes metastasis of nasopharyngeal carcinoma through induction of epithelial–mesenchymal transition and activation of AKT signaling, Carcinogenesis 33 (2012) 1302–1309.
[35] J. Ibrini, S. Fadel, R.S. Chana, N. Brunskill, B. Wagner, T.S. Johnson, A.M. El Nahas, Albumin-induced epithelial mesenchymal transformation, Nephron Exp. Nephrol. 120 (2012) e91–e102.
[36] W. Zhu, C.M. Nelson, PI3K regulates branch initiation and extension of cultured mammary epithelia via Akt and Rac1 respectively, Dev. Biol. 379 (2013) 235–245.
[37] Y. Takuwa, Y. Okamoto, K. Yoshioka, N. Takuwa, Sphingosine-1-phosphate signaling in physiology and diseases, Biofactors 38 (2012) 329–337.
[38] A. Hall, Rho GTPases and the control of cell behaviour, Biochem. Soc. Trans. 33 (2005) 891–895.
[39] H. Ungefroren, S. Sebens, K. Giehl, O. Helm, S. Groth, F. Fandrich, C. Rocken, B. Sipos, H. Lehnert, F. Gieseler, Rac1b negatively regulates TGF-beta1-induced cell motility in pancreatic ductal epithelial cells by suppressing Smad signalling, Oncotarget 5 (2013) 277–290.
[40] L. Gambardella, S. Vermeren, Molecular players in neutrophil chemotaxis–focus on PI3K and small GTPases, J. Leukoc. Biol. 94 (2013) 603–612.